

Supporting Information

An on-the-fly surface-hopping program JADE for nonadiabatic molecular dynamics of poly-atomic systems: implementation and applications

Likai Du^{†‡§}, Zhenggang Lan^{*†‡§}

[†] Key Laboratory of Biobased Materials, Qingdao Institute of Bioenergy and Bioprocess Technology, Chinese Academy of Sciences, Qingdao, 266101 Shandong, People's Republic of China

[‡] University of Chinese Academy of Sciences, Beijing 100049, People's Republic of China

[§] The Qingdao Key Lab of Solar Energy Utilization and Energy Storage Technology, Qingdao Institute of Bioenergy and Bioprocess Technology, Chinese Academy of Sciences, Qingdao, 266101 Shandong, People's Republic of China.

* Corresponding Author: Fax: +86-532-80662778; Tel: +86-532-80662630;

E-mail: lanzg@qibebt.ac.cn

1. Details about the JADE Package

The JADE package are primarily used for simulations of ultrafast processes (femtosecond to picosecond time scale) in photoexcited molecules. Currently, the JADE package is public accessible at *github.com* (a web-based Git repository hosting service). People who are interesting with the JADE program is direct to <http://github.com/jade-package>. A stable version of the JADE source code with the capability in this manuscript can be directly downloaded or by simply entering a *git clone* command. Since the JADE program is at the stage of rapid development, people are also welcomed to contact the authors to require the code with more features. The installation and usage were provided along with the source code.

Here, we give a brief introduction of the input in the program. The *keywords* to control the dynamics procedure in JADE are organized with Fortran *namelist*, and supported by both Fortran and Python modules. Most of commonly used namelist variables are *&control*, *&quantum*, *&langevin* etc. For example, a typical configure input of the TSH dynamics is given below. Restart of the simulation is possible by setting *label_restart* to 1.

```
&control
dyn_method = 201,
ntime = 1000,
dtime = 0.2,
ntime_ele = 100,
n_sav_stat = 1,
n_sav_traj = 1,
n_state = 3,
md_state_list = "1, 2, 3",
i_state = 3,
seed_random = 2014,
cor_dec = 0.1,
label_nac_phase = 1,
label_reject_hops = 1,
hop_e = 10,
label_read_velocity = 0,
label_restart = 0,
/
&quantum
qm_method = 11,
qm_package = 101,
/
```

If the Langevin dynamics is required, the following keywords can be given.

```
&langevin
gamma0 = 0.001
temperature = 300.0
/
```

The algorithm of the TSH dynamics could be summarized as follows.

1. Prepare the initial nuclear coordinates and velocity, i.e. Wigner sampling (*sampling.py* in JADE); and set up the initial electronic state (*i_state* keyword in JADE).
2. Time propagation of coordinates and velocities on the selected PES (*jade.exe* in JADE).
3. Computation of energies, gradients, and nonadiabatic coupling vectors of all relevant states at

new position and velocity.

4. Time propagation of quantum amplitudes; compare the random number with computation of hopping probabilities.
5. If hopping is performed: velocity adjustment and update of the active PES for molecular dynamics.
6. Back to point 2.
7. Statistical analysis of the dynamics results (*statistical analysis tools* in JADE)

2. Technical details of numerical NAC couplings at TDDFT level

The electronic propagation requires the numerical integration of the time-dependent Schrödinger equation (TDSE), with finite size of time steps. The simulation of nonadiabatic TSH dynamics in the adiabatic representation requires the treatment of population transfer around the points of degeneracy between electronic states. The nonadiabatic coupling matrix elements were obtained based on the numerical differentiation of the wave function in time.

$$\sigma_{ji} = \left\langle \Psi_i^*(t) \left| \frac{\partial}{\partial t} \right| \Psi_j(t) \right\rangle \quad (\text{S1})$$

A practice choice is to evaluate the numerical nonadiabatic couplings and calculate the derivative of electronic wavefunction with respect to time (S. Hammes-Schiffer, J. Tully, J. Chem. Phys. 1994, 101, 4657). In practice, the finite difference scheme was used to evaluate the NAC matrix elements, which is particularly suitable if the nonadiabatic coupling terms cannot be directly calculated using quantum chemical methods

$$\sigma_{ji} \left(t + \frac{\Delta t}{2} \right) = \frac{\left\langle \Psi_i^*(t) \left| \Psi_j(t + \Delta t) \right\rangle - \left\langle \Psi_i^*(t + \Delta t) \left| \Psi_j(t) \right\rangle \right.}{2\Delta t} \quad (\text{S2})$$

Where Δt is the time step used for the integration of the classical Newton' s equations of motion. In this approach, the true change in the electronic wave functions over the entire time step is resolved by computing overlap integrals between the adiabatic wavefunctions at time t and $t+\Delta t$ (R. Mitrić, J. Chem. Phys. 2008, 129, 164118). Our implementation of numerical nonadiabatic couplings in JADE package is based on localized atomic basis sets.

Since in the linear response TDDFT method the time-dependent electron density contains only contributions from single excitations from the manifold of the occupied to virtual KS orbitals, a natural ansatz for the excited state electronic wave function in terms of a configuration interaction with singles CIS like expansion can be formulated,

$$\left| \Psi_K(\mathbf{r}; \mathbf{R}(t)) \right\rangle = \sum_{i,a} c_{i,a}^K \left| \Phi_{ia}^{CSF}(\mathbf{r}; \mathbf{R}(t)) \right\rangle \quad (\text{S3})$$

Where $\left| \Phi_{ia}^{CSF}(\mathbf{r}; \mathbf{R}(t)) \right\rangle$ represents the singlet spin adapted configuration state function (CSF), defined as linear combinations of the Slater determinants. In order to calculate the nonadiabatic couplings according to Eq. 4 the overlap between two CI wave functions at times t and $t+\Delta t$ is needed,

$$\begin{aligned} & \left\langle \Psi_K(\mathbf{r}; \mathbf{R}(t)) \left| \Psi_I(\mathbf{r}; \mathbf{R}(t + \Delta t)) \right\rangle \right. \\ &= \sum_{ia} \sum_{i'a'} c_{i,a}^* c_{i',a'}^I \left\langle \Phi_{ia}^{CSF}(\mathbf{r}; \mathbf{R}(t)) \left| \Phi_{i'a'}^{CSF}(\mathbf{r}; \mathbf{R}(t + \Delta t)) \right\rangle \right. \end{aligned} \quad (\text{S4})$$

The overlap of the CSFs can be expressed in terms of singly excited Slater determinants

$$\left| \Phi_{ia}^{CSF}(\mathbf{r}; \mathbf{R}(t)) \right\rangle = \frac{1}{\sqrt{2}} \left(\left| \Phi_{ia}^{\alpha\beta}(\mathbf{r}; \mathbf{R}(t)) \right\rangle + \left| \Phi_{ia}^{\beta\alpha}(\mathbf{r}; \mathbf{R}(t)) \right\rangle \right) \quad (\text{S5})$$

The matrix elements of Slater determinants can be written as

$$\langle \Phi^\alpha(\mathbf{r}; \mathbf{R}(t)) | \Phi^\beta(\mathbf{r}; \mathbf{R}(t + \Delta t)) \rangle = \mathbf{det} \{ \langle \phi_k(t) | \phi'_k(t + \Delta t) \rangle \} \quad (\text{S6})$$

Where, ϕ_k, ϕ'_k are two Kohn-Sham orbitals at time t and $t + \Delta t$. The spatial KS orbitals can be expressed in terms of atomic basis functions according to

$$\langle \phi_i(t) | = \sum_{k=1}^n c_{ik}(t) \langle \chi_k(\mathbf{R}(t)) | \quad (\text{S7})$$

$$| \phi'_j(t + \Delta t) \rangle = \sum_{m=1}^n c'_{jm}(t + \Delta t) | \chi'_m(\mathbf{R}(t + \Delta t)) \rangle \quad (\text{S8})$$

And $\chi_k(\mathbf{R}(t)), \chi'_m(\mathbf{R}(t + \Delta t))$ are the related Gaussian basis functions, $c_{ik}(t), c'_{jm}(t + \Delta t)$ are the corresponding molecular orbital (MO) coefficients, respectively. One should note that $\chi_k(\mathbf{R}(t)), \chi'_m(\mathbf{R}(t + \Delta t))$ are center at different positions, and thus do not form an orthonormal basis set. Therefore, the final overlap integral of two spatial KS orbitals at time t and $t + \Delta t$ is given as

$$\langle \phi_i(t) | \phi'_j(t + \Delta t) \rangle = \sum_{k=1}^n \sum_{m=1}^n c_{ik}(t) c'_{jm}(t + \Delta t) \langle \chi_k(\mathbf{R}(t)) | \chi'_m(\mathbf{R}(t + \Delta t)) \rangle \quad (\text{S9})$$

3. Dimensionless normal coordinates

In JADE code, the dimensionless normal coordinates are used in the initial sampling procedure. The standard normal approximation defines the normal mode coordinate q and its conjugated momentum p . Then, in the atomic unit the Hamiltonian is given by

$$H = \frac{1}{2} p^2 + \frac{1}{2} \omega^2 q^2 . \quad (\text{S10})$$

It is possible to define the so-called “dimensionless” normal coordinates Q by

$$Q = \sqrt{\omega} q \quad (\text{S11})$$

Then the Hamiltonian is given by

$$H = \frac{1}{2} \omega (P^2 + Q^2) , \quad (\text{S12})$$

where P is the conjugated momentum of Q .

The employment of dimensionless normal coordinates provide is very convenient in the sampling. For example, in the atomic unit the Wigner distribution function for the ground vibrational level becomes

$$\rho_w (Q, P) = N \exp(-Q^2 - P^2) \quad (\text{S13})$$

where N is the normalization factor. In addition, Eq 21-22 in the manuscript can be easily derived if we assume that the classical energy corresponds to the quantum energy of a vibrational level

$$H = \frac{1}{2} \omega (P^2 + Q^2) = \omega (n + \frac{1}{2}) . \quad (\text{S14})$$

This relationship finally gives

$$P^2 + Q^2 = 2n + 1 \quad (\text{S15})$$

4. Examination of Several Setup Parameters in the Electronic-Structure Calculations

Here, we also try to examine several parameters in the electronic-structure calculations, i.e. the Casida's assignment ansatz, the output accuracy of the electronic structure calculations, and the dependence of functionals. In the following TSH dynamics, the trajectories start from the $\pi \pi^*$ state (S_2) of CH_2NH_2^+ molecule. The nuclear equations of motion are integrated with a time step of 0.2 fs, and the electronic amplitude is propagated with a time step of 0.002 fs. The results were obtained by averaging 100 trajectories.

According to Casida's assignment ansatz, the expansion coefficients for the configurations of the excited state can be obtained from \mathbf{X} and \mathbf{Y} vectors in TDDFT calculations. Thus, we evaluated several variations to define the expansion coefficients, which are (1) $\mathbf{X}+\mathbf{Y}$ scaled by pre-factor (Eq. (18) in the main manuscript), (2) \mathbf{X} scaled by pre-factor, (3) $\mathbf{X}+\mathbf{Y}$, (4) \mathbf{X} . For each option, the TSH dynamics simulation of CH_2NH_2^+ molecule was performed with the same dynamic parameters mentioned above. Interestingly, the fractional occupation for each state is similar for different options (Figure S1). In summary, the results from different assignment options appear to be consistent in the TSH dynamics

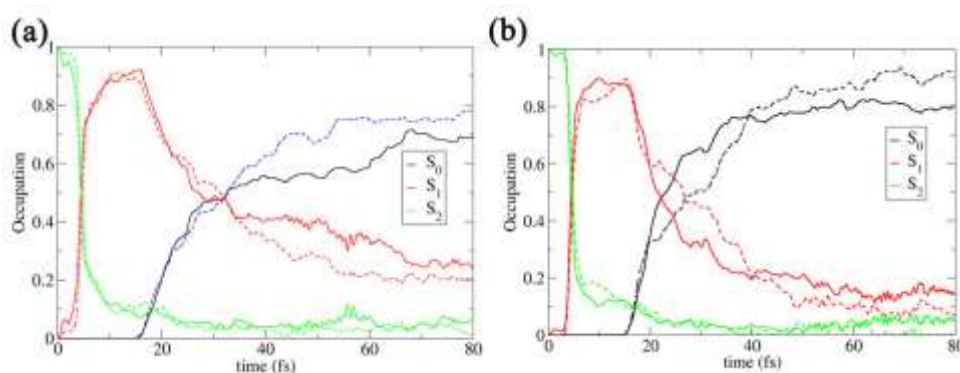


Figure S1. The average fractional occupation for the CH_2NH_2^+ as the function of time (fs). (a) scaled $\mathbf{X}+\mathbf{Y}$ (straight line) and scaled \mathbf{X} (dashed line); (b) $\mathbf{X}+\mathbf{Y}$ (straight line) and \mathbf{X} (dashed line).

The on-the-fly TSH dynamics method requires the computations of molecular orbitals, energies, gradients, and CI coefficients from the QC packages. Here, we

provided an analysis of the numerical stability of TSH dynamics on the output accuracy of the electronic structure calculations. For the CH_2NH_2^+ molecule, the TSH dynamics simulations were performed in two conditions, in which, the output in electronic structure calculations is round up to (1) 8 decimals, and (2) 4 decimals. As shown in Figure S2a, no qualitative differences were observed in the population dynamics. Thus, TSH dynamics is not very sensitive to the output accuracy of QC packages.

The quality of the TDDFT solutions is directly related to the standard approximations for xc-functionals. Thus, TSH dynamics simulation for the CH_2NH_2^+ molecule were performed with B3LYP and the range-separated CAM-B3LYP functional. And the 6-31G** basis set were used. As shown in Figure S2b, the decay of the fractional occupations of S_1 and S_2 states seems to be slower at the CAM-B3LYP level. This slightly difference may arise from the possible charge transfer characters in the CH_2NH_2^+ molecule. This also indicates that one should be careful on the charge transfer problem in TDDFT method.

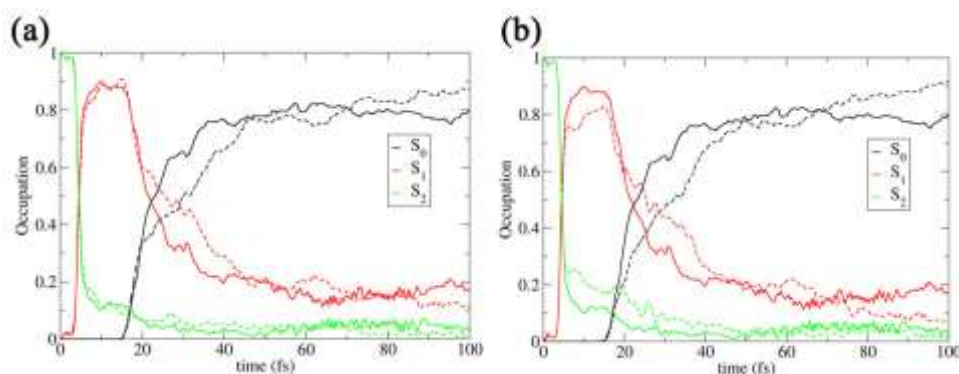


Figure S2. The average fraction of trajectories for the CH_2NH_2^+ molecule as function of time (fs) starting at S_2 state. (a) high accuracy (straight line) and lower accuracy (dashed line) (b) B3LYP (straight line) and CAM-B3LYP (dashed line).

5. The Photoinduced Relaxation of $\text{CH}_2\text{NH}_2^+\cdot 3\text{H}_2\text{O}$ complex

The photo-induced dynamics of CH_2NH_2^+ molecule may be different in the explicit solvent. Here, we suppose that the main impact of the solvation on the excited-state evolution is due to the few water molecules directly hydrogen bonded to CH_2NH_2^+ molecule. Our optimization indicates that at the most only about 3 water molecules were able to directly interact with CH_2NH_2^+ . Then, we optimized various structures of $\text{CH}_2\text{NH}_2^+\cdot 3\text{H}_2\text{O}$ complex, and the most stable geometry were given in Figure S3a. On the basis of the optimized groundstate geometry, the TSH dynamics, starting from the S_2 state, is performed at TDDFT/CAM-B3LYP/6-31G** level, interfaced with Gaussian 09 package. The LD scheme was also applied with $\gamma = 50 \text{ ps}^{-1}$, which is related to the viscosity of water molecules. The temperature was set to 300 K in LD scheme. The water molecule would fly away in the dynamics simulation without friction, thus, only the dynamics results with LD scheme is reported here.

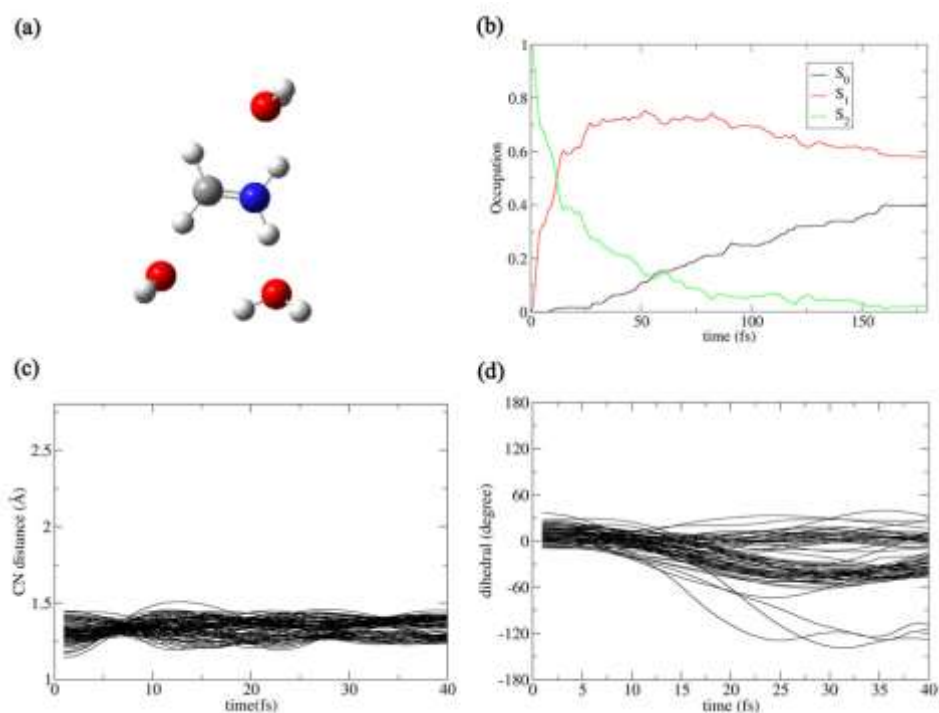


Figure S3. (a) The stable geometry of $\text{CH}_2\text{NH}_2^+\cdot 3\text{H}_2\text{O}$ complex; (b) Average fraction of trajectories for each state; (c) the evolution of the CN distance as a function of time (fs); (d) the evolution of the twisted angle distance as a function of time (fs)

As shown in Figure S3b, the lifetime of the S_2 state is estimated to be ~ 20 fs, which is longer than the isolated case (~ 10 fs). This may attribute to hydrogen bonded interactions between CH_2NH_2^+ and water molecules. The $\text{CH}_2^+ \dots \text{NH}_2$ dissociation pathway was strongly prohibited when the explicit water molecules are involved (Figure S3c). And most significant motion is the twisted motion of CH_2NH_2^+ . This behavior is consistent to the LD simulation result ($\gamma = 100 \text{ ps}^{-1}$) of the CH_2NH_2^+ molecule without explicit solvents (Figure 3d). In addition, the water molecules may fly away from the CH_2NH_2^+ molecule in the simulated time scale.

6. Photo-induced Relaxation of of Fullerence (C_{20}) Starting at S_3 State

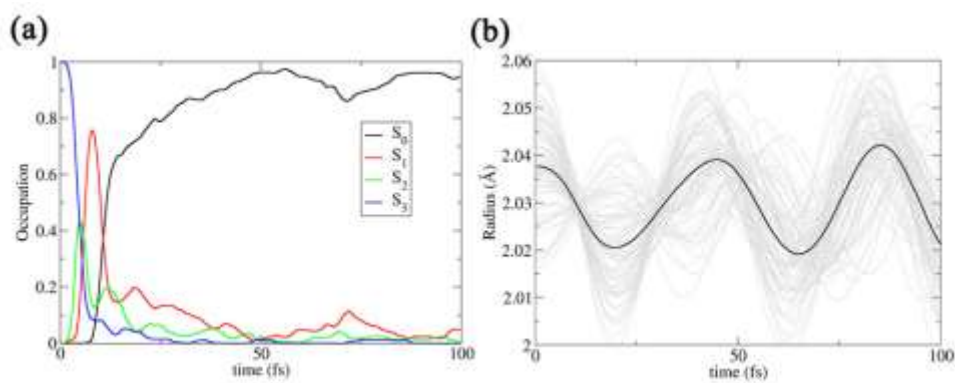


Figure S4. (a) Time-dependent fractional occupation for C_{20} system, starting from S_3 state; (b) the radius of C_{20} molecule as a function of time (fs), average radius was given in black line.